

Essential role of membrane vesicles for biological activity of the bacteriocin micrococcin P1

Yao Liu¹ | Qian Liu¹ | Lu Zhao² | Seth W. Dickey³ | Hua Wang¹ | Rui Xu⁴ |
Tianchi Chen¹ | Ying Jian¹ | Xi Wang¹ | Huiying Lv¹ | Michael Otto³  | Min Li^{1,5}

¹Department of Laboratory Medicine, Ren Ji Hospital, Shanghai Jiao Tong University School of Medicine, Shanghai, China

²Research Center for Marine Drugs, State Key Laboratory of Oncogenes and Related Genes, Department of Pharmacy, Ren Ji Hospital, Shanghai Jiao Tong University School of Medicine, Shanghai, China

³Pathogen Molecular Genetics Section, Laboratory of Bacteriology, National Institute of Allergy and Infectious Diseases, U.S. National Institutes of Health, Bethesda, Maryland, USA

⁴Institute of Molecular Medicine and Shanghai Key Laboratory for Nucleic Acid Chemistry and Nanomedicine, State Key Laboratory of Oncogenes and Related Genes, Ren Ji Hospital, Shanghai Jiao Tong University School of Medicine, Shanghai, China

⁵Faculty of Medical Laboratory, Science, Shanghai Jiao Tong University School of Medicine, Shanghai, China

Correspondence

Michael Otto, 50 South Drive, Bethesda, MD 20814, USA

Email: motto@niaid.nih.gov

Min Li, 160 Pujian Road, Shanghai 200127, China

Email: rjlimin@shsmu.edu.cn

Funding information

Shanghai Committee of Science and Technology, Grant/Award Number: 19JC1413005; National Natural Science Foundation of China, Grant/Award Numbers: 81873957, 82172325; Division of Intramural Research, National Institute of Allergy and Infectious Diseases, Grant/Award Number: AI000904

Abstract

Bacterial membrane vesicles (MVs) have recently gained much attention and have been shown to carry a wide diversity of secreted bacterial components. However, it is poorly understood whether MV carriage is an indispensable requirement for a cargo's function. Bacteriocins as weapons of bacterial warfare shape the composition of microbial communities. Many bacteriocins have pronounced hydrophobicity that is imposed by their mechanism of action, but how they diffuse through aqueous environments to reach their target competitors is not known. Here we show that antimicrobial competitive activity of an exemplary hydrophobic bacteriocin of the thiopeptide antibiotic family, micrococcin P1 (MP1), is dependent on incorporation into MVs, which were found to carry MP1 at high concentrations. In contrast, MP1 without MV association was poorly active due to low solubility. Furthermore, we provide previously unavailable evidence that MVs fuse with a Gram-positive bacterium's cytoplasmic membrane, in this case to deliver a bacteriocin to its intracellular target. Our findings demonstrate how bacteria overcome the problem associated with secreting hydrophobic small molecules and delivering them to their target and show that MVs have a key function in bacterial warfare. Furthermore, our study provides hitherto rare evidence that MVs provide an essential rather than merely accessory function in bacterial physiology.

KEYWORDS

bacterial competition, bacteriocins, gram-positive bacteria, membrane vesicles, *Staphylococcus*

1 | INTRODUCTION

Bacteria represent an important part of the human microbiome. They have a multi-faceted and often beneficial relationship with the human host, for example producing vitamins, helping digestion, and fighting off pathogens, while others may also cause disease (Cho & Blaser, 2012; Human Microbiome Project, C, 2012). In addition, they interact with each other in a variety of

This is an open access article under the terms of the [Creative Commons Attribution-NonCommercial-NoDerivs License](https://creativecommons.org/licenses/by-nc-nd/4.0/), which permits use and distribution in any medium, provided the original work is properly cited, the use is non-commercial and no modifications or adaptations are made.

© 2022 The Authors. *Journal of Extracellular Vesicles* published by Wiley Periodicals, LLC on behalf of the International Society for Extracellular Vesicles

ways. These can be mutually beneficial, but often – at least in nutrient-limited environments such as the skin – are competitive (Faust et al., 2012; Liu, Du et al., 2020; Liu, Meng et al., 2020; Nakatsuji et al., 2017; Paharik et al., 2017; Woyke et al., 2006). Many bacterial strains produce bacteriocins, which are peptides or small proteins directly aimed to kill competitors (Riley & Wertz, 2002). Often, bacteriocins have considerable hydrophobicity, which is linked to their mechanism of action. This is because many bacteriocins function by either forming pores in cytoplasmic membranes, interfering with essential membrane-bound cell-wall precursors such as lipid II, or need to pass through the membrane of the target organism to reach intracellular targets such as the protein or DNA synthesis machinery (Ciufolini & Lefranc, 2010; Grein et al., 2019; Héchard & Sahl, 2002; Moll et al., 1999; Towle & Vederas, 2017). However, it has remained poorly understood how hydrophobic bacteriocins manage to remain soluble through an aqueous environment to reach the target organism and exert their antimicrobial activity (Chan & Burrows, 2021).

Membrane vesicles (MVs) are lipid membrane nanoparticles originally found in Gram-negative bacteria, where they have also been called outer membrane vesicles (OMVs), because they originate from blebbing of the outer membrane (Schwechheimer & Kuehn, 2015). Later, they were also described in Gram-positive bacteria, which was an astounding finding given that they need to pass the compact and thick cell wall of Gram-positive bacteria. To this date it remains unknown how exactly this is accomplished, but recent evidence obtained in *Bacillus subtilis* suggests that enzymes that digest the cell wall are involved in a process possibly linked to cell death (“bubbling cell death”) (Abe et al., 2021; Brown et al., 2015; Toyofuku et al., 2017, 2019). Furthermore, in *Staphylococcus aureus*, MV formation appears to involve membrane-active peptides, the phenol-soluble modulins (PSMs) (Schlatteer et al., 2018; Wang et al., 2018).

Nowadays, it is believed that the production of MVs is at least nearly ubiquitous in bacteria. MVs range in size from 20 to 400 nm in diameter and are naturally filled with contents such as nucleic acids (Koeppen et al., 2016), toxins (Chatterjee & Chaudhuri, 2011), signaling molecules (Toyofuku et al., 2017), enzymes (Lekmeechai et al., 2018), and antibiotic resistance factors (Ciofu, 2000). Bacterial MVs have recently garnered much attention and have been associated with diverse functions, such as in nutrient acquisition, quorum-sensing, and biofilm formation, in addition to various further roles in pathogenesis (Caruana & Walper, 2020; Ellis & Kuehn, 2010). Furthermore, MVs can be recognized by or even fuse with host immune cells, modulating immune responses (Bitto et al., 2021; Kaparakis-Liaskos & Ferrero, 2015), and potentially be used as vaccines or vaccine adjuvants (Wang et al., 2019). However, except for a likely essential function in quorum-sensing of particularly hydrophobic quorum-sensing signal molecules in *Pseudomonas aeruginosa* (Mashburn & Whiteley, 2005) and other Gram-negative bacteria (Toyofuku et al., 2017), it remains unclear if MVs provide essential functions to any identified cargo. This is because the corresponding soluble substances found to be included in MVs are also functional without MVs, which includes the reported pro-inflammatory roles of MVs that are based on soluble agents such as nucleic acids (Bitto et al., 2021) as well as bacterial antagonistic interactions that have been attributed to the delivery of harmful enzymes to the surface of competitors (Kadurugamuwa & Beveridge, 1996). MVs have been suggested as delivery tools for hydrophobic bacteriocins in therapeutic applications (Arthur et al., 2014; Niaz et al., 2019), and bacteriocins can be found among the multitude of proteins that are associated with MVs, as shown for example in a strain of *Lactobacillus acidophilus* (Dean et al., 2019). Furthermore, the pigment violacein, which also has antibiotic and bactericidal properties, has recently been shown to be MV-associated (Choi et al., 2020). However, there is not much evidence supporting the notion that MVs play a key role in bacterial competition. Furthermore, regarding both a potential application of MVs as delivery tools as well as in bacterial competition, it is not understood how MVs can deliver embedded compounds to a target Gram-positive bacterium, which is of particular importance given that this class of bacteria contains a large number of notoriously antibiotic-resistant pathogens, such as *S. aureus*, *Streptococcus* spp. and *Enterococcus* spp., to name but a few (Fischetti et al., 2019).

In the present study, we developed and evaluated the hypothesis that MVs are essential for hydrophobic bacteriocins to be active, particularly in the context of bacterial competitive interaction. To that end, we chose to investigate the thiopeptide bacteriocin, micrococcin PI (MPI). MPI is an inhibitor of protein synthesis initiation (Ciufolini & Lefranc, 2010) that is produced by several strains of Gram-positive bacteria including *Staphylococcus hominis* S34 (Ciufolini & Lefranc, 2010; Liu, Du et al., 2020). We chose MPI because it has (i) a demonstrated role in bacterial interaction within the human microbiome (Liu, Du et al., 2020), (ii) strong antimicrobial activity against Gram-positive bacteria (Ciufolini & Lefranc, 2010), and (iii) like the entire family of thiopeptide antibiotics, high hydrophobicity and low solubility in aqueous solutions that underlies the need for solubilization for example by nanoparticles for their potential therapeutic application (Chan & Burrows, 2021; Ciufolini & Lefranc, 2010; Liu, Du et al., 2020).

2 | MATERIALS AND METHODS

2.1 | Bacterial strains and growth conditions

The *S. aureus* target strain used in our study was CA-MRSA (ST59) strain RJ-2 (Li et al., 2016; Liu, Du et al., 2020). The *Acinetobacter baumannii* strain used was *A. baumannii* ATCC19606. S34-1 is a commensal *S. hominis* strain that produces MPI (Liu, Du et al., 2020). Strain ΔS34-1 is a transposon mutant that carries a transposon insertion in the structural MPI gene, *tclE*

(Liu, Du et al., 2020). Growth of strains S34-1 and Δ S34-1 is indistinguishable (Liu, Du et al., 2020). Bacteria were generally grown in LB (*A. baumannii*) or tryptic soy broth (TSB; Oxoid; all other bacteria) with shaking at 200 rpm at 37°C.

2.2 | Micrococcin P1

Micrococcin P1 (MP1) was purchased from Cayman Chemical (Ann Arbor, MI, USA; item number 17093; \geq 95% purity).

2.3 | Agar diffusion assay

An overnight culture of *S. aureus* was diluted in melted TSA to an OD₆₀₀ of 0.0008 and then poured into Petri dishes for solidification. MP1 was diluted in double-distilled water to a final concentration of 1.128 μ g/ml. The 4 \times concentrated supernatants of S34-1 wild type (WT) and Δ S34-1 were prepared as previously described (Liu, Du et al., 2020). Three microlitre of overnight cultures or supernatants of *S. hominis* S34-1 or Δ S34-1 strains, or pure MP1 solution were dropped onto the bacterial lawn. The plates were incubated at 37°C for 16–24 h and evaluated for inhibition zones.

2.4 | Size-based culture filtrate separation and inhibition assay

Overnight cultures of *S. hominis* S34-1 and Δ S34-1 were inoculated into conical flasks containing 50 ml TSB to the same OD₆₀₀ of 0.028 and cultivated for different hours, as indicated. For each time point and strain one flask was used. To collect culture filtrate, cultures were centrifuged at 5000 \times g at 4°C for 10 min, and the supernatants were sterile-filtered twice using 0.22- μ m filters. Twelve millilitre of sterile-filtered supernatants were transferred onto sterile 50-kDa ultrafiltration tubes (Millipore) and centrifuged at 5000 \times g and 4°C to gain a 20-fold concentrated concentrate. Untreated supernatants or a tenth of either >50-kDa retentate or <50-kDa filtrate were added to suspensions containing the same number of *S. aureus* (1×10^7 CFU). The growth of *S. aureus* was measured every hour for 8 h.

2.5 | MV isolation

MVs were isolated by modification of the technique described previously for the recovery of *S. aureus* vesicles from culture supernatants (Lee et al., 2009). Overnight-cultured cells of *S. hominis* (S34-1 and Δ S34-1) were inoculated into fresh TSB with 1:100 dilution and grown for 8 h (except for the test of MV yields at different cultivation times from 2 to 22 h) at 37°C with shaking at 200 rpm. Cell cultures were centrifuged for 10 min at 8000 \times g and the supernatants were filtered through a 0.22- μ m pore-size filter. The filtrate was then concentrated by ultrafiltration using a 50-kDa hollow-fiber membrane (Millipore). Then, the crude MVs were obtained by ultracentrifugation of the above filtrate at 174,900 \times g at 4°C for 8 h in a SW 32Ti rotor (Beckman Coulter). The pellets were suspended in 4.4 ml 50% OptiPrep solution (Axis-Shield) and applied to the bottom of 4 ml 40% and 1.6 ml 10% OptiPrep solutions. After centrifugation at 200,000 \times g for 5 h at 4°C in a SW 41Ti rotor, ten fractions of equal volume of 1 ml or the visible band between 10% and 40% gradients was collected. The MV yield was $\sim 1 \mu$ g per ml of 8-h culture filtrate.

2.6 | Nanoparticle tracking analysis (NTA)

Nanoparticles in the isolated MV suspensions were analyzed using a NanoSight NS300 (Malvern) instrument equipped with a 488-nm laser and a sCMOS camera. The platform was cleaned with sterile PBS to ensure no residue was present and to remove any potential air bubbles before analyzing samples. All samples were diluted in PBS to a final volume of 1 ml and injected into the sample chamber with sterile syringes, yielding particle concentrations of 10^8 particles per milliliter in accordance with the manufacturer's recommendations. The software used for capturing and analyzing the data was the NTA 3.4 Build 3.4.003. For each measurement, the camera level was adjusted to 14.

2.7 | Transmission electron microscopy (TEM) imaging

Generally, 10 μ l of MV solution was dropped onto a copper grid, let to sit for 7 min and wiped dry. A drop of uranyl acetate (3%) was added to the sample to stain for 10 s. The grid was then washed by PBS twice and dried at room temperature for about 5 min before being put on the microscope. Electron micrographs were recorded with a HT7700 microscope (Hitachi) at 100 kV

acceleration voltage. To take TEM pictures of the 10 fractions collected from the density-gradient ultracentrifugation, sterile PBS was first used to wash the fractions. To that end, the fractions were centrifuged at $200,000 \times g$ at 4°C for 3 h in a type 41Ti rotor and the pellets were then resuspended in 1 ml of PBS.

2.8 | TEM with immunogold labeling

Isolated MVs were labeled with 100 mg/ml FITC isomer I (TCI) for 1 h at room temperature and washed with PBS by ultracentrifugation at $200,000 \times g$ at 4°C for 3 h for three times. The labeled MVs were resuspended in PBS. 1×10^8 *A. baumannii* or *S. aureus* cells were incubated with 20 μg of FITC-labeled MVs at 37°C for 50 min and then washed twice with and resuspended in PBS. The samples were dropped onto copper grids that had been treated with 0.01% poly-L-lysine in PBS (Sangon), let to rest for 5 min, and then fixed in 4% paraformaldehyde/PBS (Sangon) for 20 min. The grids were washed twice with PBS, followed by incubation for 30 min with 3% BSA/PBS (Sangon) to block non-specific reactions. After washing with PBS twice, the grids were incubated with rabbit anti-FITC antibody (Sangon) for 1 h, washed three times with PBS, and incubated for 1 h with colloidal gold (20 nm)-labeled anti-rabbit IgG (Abcam). The gold-labeled specimens were then washed with PBS three times and fixed in 4% paraformaldehyde/PBS for 20 min. After washing with PBS and staining with 1% uranyl acetate for 5 s, the samples were analyzed by TEM.

2.9 | Lipid and protein quantification

The red fluorescent dye FM 4-64 (Life Technologies) was used to stain lipids and quantify the lipid amount in MV solutions. Appropriately diluted solutions were dyed on ice for 2 min by FM4-64 with a final concentration of 5 $\mu\text{g}/\text{ml}$. Fluorescence intensity was then measured using the fluorescence microplate reader Synergy HI (Biotek) with an excitation wavelength of 558 nm and an emission wavelength of 700 nm. The protein amount of MV isolates or fractions from density gradient ultracentrifugation was determined using a bicinchoninic acid (BCA) assay according to the manufacturer's manual (Yeasen).

To visualize the protein components of different centrifugal fractions, MV samples were mixed with sample buffer, boiled at 100°C for 10 min, and then applied to a 10% SDS gel, which was stained by silver staining using the Protein Stains O kit (Sangon) according to the manufacturer's instructions.

2.10 | High-pressure liquid chromatography (HPLC) analysis and standard curve

Quantitative determination of MPI content was performed using HPLC. To that end, pure MPI solutions or in-vacuo concentrated MPI extracts (from MVs) were injected onto a YMC Pack Pro C18 RS column (5 μm pore size, 4.6×250 mm), and eluted with a gradient as follows (H_2O as eluent A, and acetonitrile as eluent B): 0–20 min, 35–65% B; 20–28 min, 65–95% B; 28–30 min, 95% B, at a flow rate of 1.0 ml/min. The standard curve was obtained by the calculations of peak-area (at ~ 12 min) versus the pure MPI concentrations. For calibration, an MPI stock solution was prepared by dissolving pure MPI in methanol to a concentration of 3 mg/ml. The stock solution was further diluted with methanol to give solutions of 10 $\mu\text{g}/\text{ml}$, 50 $\mu\text{g}/\text{ml}$, 100 $\mu\text{g}/\text{ml}$, 170 $\mu\text{g}/\text{ml}$ and 200 $\mu\text{g}/\text{ml}$, which were used for the calibration curve.

To determine the concentration of MPI in supernatants or MVs, MV solutions were first sonicated for 20 min with an ultrasonic frequency of 90 khz. Cell-free supernatants or MV solutions that were prepared in this fashion were extracted with ethyl acetate three times. The organic layers were combined and concentrated in vacuo. The resulting gum was dissolved in 500 μl methanol for HPLC analysis. Concentrations of MPI were calculated according to the calibration curve (Supplementary Figure S1).

2.11 | RNA extraction and quantitative real-time polymerase reaction (qRT-PCR)

Total RNA was extracted using RNeasy[®] kits (Qiagen) according to the manufacturer's instructions, checked for purity, and concentration was assessed using a NanoDrop spectrophotometer (Thermo Scientific). A total of 0.5 μg RNA was reverse-transcribed to cDNA using a QuantiTect[®] kit (Qiagen). For real-time PCR, which was performed on a LightCycler96 qPCR system (Roche), each 20- μl reaction contained 10 μl of SYBR green mix (Roche), 0.1 μl of specific primers (Supplementary Table S1) at concentrations of 100 μM , 7.8 μl of highly purified H_2O , and 2.0 μl of template. Expression levels of evaluated genes were calculated using the $2^{-\Delta\Delta\text{CT}}$ method. For the evaluation of transcriptional expressions of cytokines and the main synthetic genes of MPI (Bennallack et al., 2014), each value was corrected for the expression of the housekeeping gene *GAPDH* or *gyrB*, respectively, and compared to the control condition.

2.12 | Inhibitory activity of culture filtrates and MVs at different times of growth

Three hundred millilitre of supernatants of *S. hominis* S34-1 and Δ S34-1 were collected at different time points from 2 to 22 h of growth. Fifteen millilitre of the supernatants were stored for supernatant inhibition assays while the rest was operated for MV isolation. For the comparison of inhibitory activities of MVs and supernatants over the course of growth, 400 μ l of sterile supernatants and 60 μ l of MV solutions were added to 4 ml of *S. aureus* dilutions containing 1×10^7 CFU. The growth of *S. aureus* was measured by determining the OD600. The experiment was performed three times and inhibition abilities were calculated by subtracting the corresponding OD600 value of the S34-1 group from those of the Δ S34-1 group.

2.13 | Test for vesicle-mediated transfer of antimicrobial activity to target bacteria

Overnight cultures of *A. baumannii* ATCC19606 and *S. aureus* strain ST59 RJ-2 were subcultured (1:100) in fresh LB and TSB, respectively, and grown for 5 h. After centrifugation at $5000 \times g$ for 5 min, cells were washed twice with sterile PBS and resuspended in PBS with 0.2% glucose. Twenty microgram of S34-1 MVs or the same volume of PBS were incubated with 1×10^8 bacterial cells at 37°C for 50 min. After the incubation, samples were washed three times with PBS and resuspended in 700 μ l of PBS and then placed into 2-ml FastPrep tubes (MP Biomedicals). Tubes were placed into the FastPrep-96 instrument and run for two 60-s intervals at a speed setting of 14,000 rpm/min. After the lysis process, tubes were centrifuged at $5000 \times g$ at 4°C for 5 min. A total of 650 μ l of supernatant was transferred to a new tube and extracted by the same volume of ethyl acetate three times. The organic extractions were concentrated in vacuo and dissolved in 50 μ l of methanol. Ten microlitre of each sample was dropped onto the *S. aureus* lawn to detect antimicrobial activity (presence of MPI).

2.14 | Confocal microscopy for MV tracking

For MV tracking, isolated MVs secreted by *S. hominis* S34-1 cells were labeled using PKH26 red fluorescent dye according to the manufacturer's manual (Sigma-Aldrich). Briefly, MVs were labeled with PKH26 dye in the dark at a concentration of 4 μ M at 37°C for 20 min. The supernatant containing unbound dye was removed by $2 \times$ ultracentrifugation at $174,900 \times g$ and subsequent density-gradient ultracentrifugation at $200,000 \times g$. All ultracentrifugation steps were performed at 4°C for 3 h. The labeled MVs were then incubated with 1×10^8 *A. baumannii* or *S. aureus* cells at 37°C for 50 min. After the incubation, samples were washed three times with PBS and resuspended in PBS containing 0.2% glucose to an OD₆₀₀ of 2.0. Cells were imaged with a TCS Sp8 confocal microscope (Leica) using a 100 \times oil objective lens.

2.15 | MV fusion with target bacterial membrane

Octadecyl rhodamine B chloride (R18, TCI) was used to monitor fusion of MVs with the bacterial membrane of a target microorganism. R18 is self-quenched when introduced into the bilayer. Upon fusion with an unlabeled target membrane, dilution of the probe will cause an increase of fluorescence. Hundred microgram of isolated MVs were labeled with R18 at a concentration of 100 μ g/ml for 1 h at room temperature. The unbound dye was removed by ultracentrifugation at $174,900 \times g$ and subsequent density-gradient ultracentrifugation at $200,000 \times g$, after which MVs were resuspended in PBS. Overnight cultures of *S. aureus* and *A. baumannii* were subcultured (1:100) in fresh TSB and LB, respectively, and grown for 5 h. Afterwards, the cells were washed three times with PBS and resuspended in PBS with 0.2% glucose. Seven microgram of labeled MVs were applied to 1×10^8 *S. aureus* or *A. baumannii* cells and fluorescence was measured for 30 min using a fluorescent plate reader (Synergy H1) with an excitation wavelength of 560 nm and an emission wavelength of 590 nm.

2.16 | MV lysis and proteinase K treatment

Hundred microlitre aliquots of MV solutions (~ 20 μ g MVs per aliquot) were pipetted into 2-ml tubes, mixed well with 60 mg glass beads (0.1 mm, Biospec) and lysed using a FastPrep-96 Sample Preparation Instrument (14,000 rpm/min for 1 min). Samples were then centrifuged at $50,000 \times g$ at 4°C for 1 min, transferred to a new 1.5-ml tube, and incubated with 20 μ g/ml proteinase K (PK, MP Biomedicals) at 37°C for 1 h. Control samples did not undergo lysis and/or PK treatment, but were mixed with beads to control for the volume loss associated with the procedure and for possible adherence to beads. The samples were analyzed by TEM and extracted by ethyl acetate, concentrated in vacuo and then used for HPLC analysis of MPI.

2.17 | Test for incorporation of MPI into *S. hominis* ΔS34-1 MVs

MPI was added to equal amounts of *S. hominis* ΔS34-1-derived MVs or the same volume of PBS to a final concentration of 1 μg MPI per ml and the resulting mixtures were shaken at 200 rpm at 37°C for 3 h. These mixtures were then applied to density-gradient ultracentrifugation at 200,000 × g at 4°C for 3 h. Afterwards, the bands between the 10% and 40% gradients were collected (~300 μl volume). Thirty microlitre of the collected bands with the original MVs, the MPI-incubated MVs, or a MPI control sample (without MVs but undergoing density-gradient ultracentrifugation) were dropped onto a test plate with an *S. aureus* lawn. 20-μg (~100-μl) aliquots of MPI-incubated MVs were further treated with proteinase K and 0.1-mm beads as described above. Samples were then first sonicated for 15 min with an ultrasonic frequency of 90 kHz and afterwards extracted with ethyl acetate three times. The resulting gum was dissolved in methanol for HPLC analysis.

2.18 | Animal study

Female BALB/c nude mice (CAnN.Cg-Foxn1^{tmu}/CrIVr, Shanghai JSJ Experimental Animal Co., Ltd.) were used for the skin abscess model. All mice were 6 weeks of age at the time of use and had access to food and water ad libitum. The ambient temperature was 20–25°C, the relative humidity was 40–70% and light-dark alternation time was 12–14/12–10 (h). The animal experiment was reviewed and approved by the ethics committee of Ren Ji Hospital, School of Medicine, Shanghai Jiao Tong University, Shanghai, China (Approval Number: RA-2020-093).

2.19 | Mouse skin abscess model

Overnight cultures of the *S. aureus* strain ST59 were subcultured (1:100) in fresh TSB and grown for 4 h. After centrifugation at 5000 × g for 5 min, cells were washed twice with and resuspended in sterile PBS. Mice were anesthetized with 2,2,2-tribromoethanol (Sigma-Aldrich) and subcutaneously inoculated with 0.1 ml of live cells (1 × 10⁸ CFUs) on the left and right flanks.

For MV treatment, the concentration of MPI in MV samples was first determined by HPLC as described above. Each skin flank received treatments with 600 ng MPI, 600 ng MPI in *S. hominis* S34-1-derived MVs (7 μg) or *S. hominis* ΔS34-1-derived MVs (7 μg), each in 100 μl of sterile PBS, via intra-abscess injection at the outlined area 1 h after MRSA inoculation. Abscesses were excised 22 h post-infection and the tissue samples were homogenized in PBS using a FastPrep-96 Sample Preparation Instrument (MP Biomedicals). RNA was extracted for the measurement of inflammatory cytokine gene expression. CFU of *S. aureus* were determined by plating ground skin tissue samples in appropriate dilution series on blood agar after incubating the plates at 37°C for 24 h. The abscess length (L) and width (W) dimensions were used to calculate the abscess area using the formula L × W. Tissue samples from each group were fixed in 4% formalin (Sangon) for 24 h at 4°C, embedded in paraffin, sectioned, and stained with hematoxylin and eosin.

2.20 | Statistical analysis

Statistical analysis was performed using GraphPad Prism 8. Anderson-Darling, D'Agostino & Pearson, Shapiro-Wilk, and Kolmogorov-Smirnov tests were used to analyze the normality of data. If all groups were equally distributed by results from all four tests, parametric (one-way ANOVA, two-tailed unpaired *t*-tests, as appropriate) were used. Otherwise, non-parametric tests were used as indicated. Data represent the mean and SD from at least three independent experiments. Values of *p* < 0.05 were considered to be statistically significant.

3 | RESULTS

3.1 | Active secreted MPI is not monomeric

To gain preliminary insight into whether MPI (Figure 1a) may be associated with MVs when secreted by its producing organism, *Staphylococcus hominis* S34-1, we tested the activity of pure MPI in comparison with culture filtrate (concentrated 4 × by lyophilization, from a culture grown for 8 h) of *S. hominis* S34-1 and *S. hominis* S34 bacteria on agar plates with embedded *S. aureus* as test target organism. For control of specificity, we also included culture filtrate and bacteria of an isogenic mutant, *S. hominis* ΔS34-1, in which the MPI structural gene has a transposon integration and no MPI is produced. While the culture filtrate

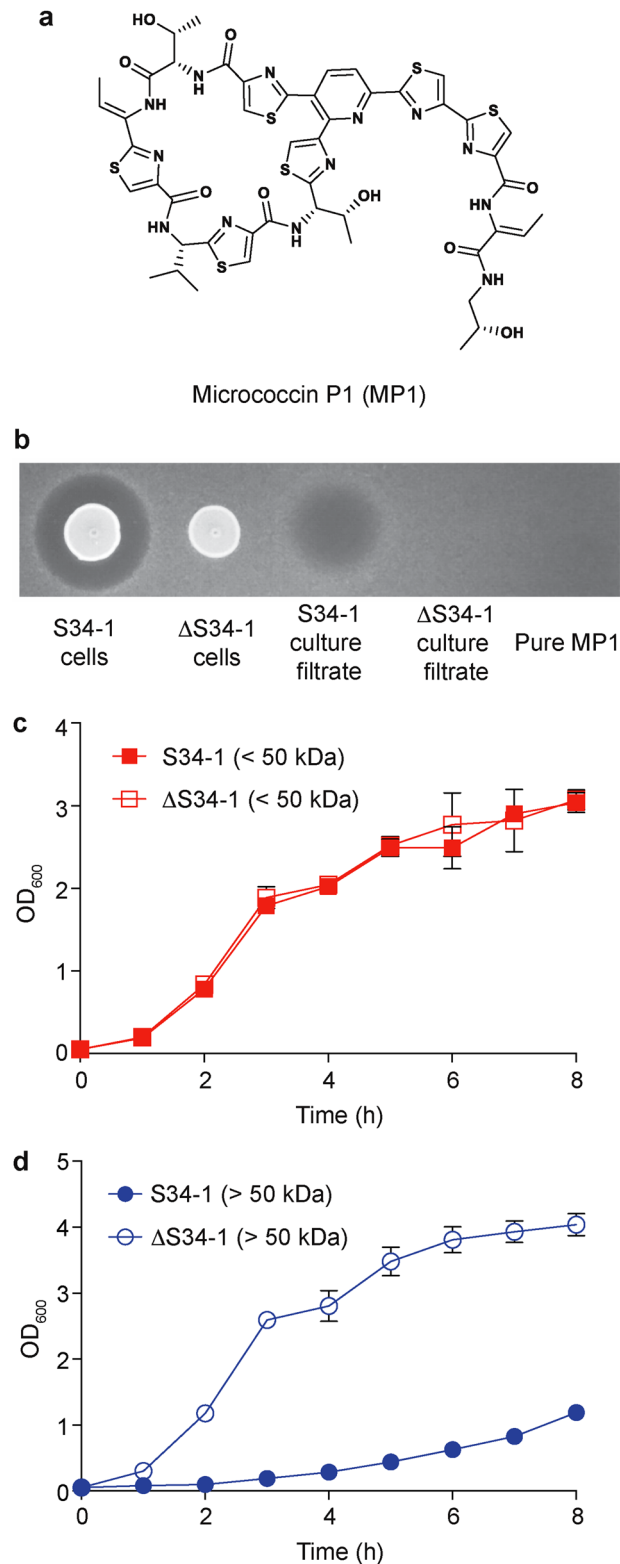


FIGURE 1 Active secreted MP1 is not monomeric. (a) Structure of MP1. (b) Activity of MP1-producing bacteria (*S. hominis* S34-1) and of an isogenic mutant (*S. hominis* Δ S34-1) without MP1 production, the corresponding culture filtrates (4 \times concentrated by lyophilization) from 8 h of growth, and a pure MP1 preparation of the same concentration as measured in the S34-1 culture filtrate (1.2 μ g/ml; see Table 1). (c, d), Activity of > and <50 kDa fractions obtained by ultrafiltration with 50 kDa cutoff devices of the *S. hominis* S34-1 and Δ S34-1 culture filtrates. Amounts corresponding to the same original volume of culture filtrate were added to *S. aureus* and growth (OD₆₀₀) was measured for 8 h. $n = 3$ /group. Error bars show the mean \pm SD

TABLE 1 MPI production during growth and association with MVs

Time/MPI concentration	Supernatant ^a (mean ± SD, µg/ml)	MV ^s ^a (mean ± SD, µg/ml)	<50 kDa fraction ^a (mean ± SD, µg/ml)	MPI percent in MV ^s ^b (Mean ± SD)	Number of MPI molecules per ml (mean)	
					Supernatant ^c	MV ^s ^d
2 h	0.103 ± 0.015	0.005 ± 0.002	0.039 ± 0.007	5.18% ± 1.86%	5.42 × 10 ¹³	1.06 × 10 ²⁰
4 h	0.253 ± 0.005	0.023 ± 0.007	0.085 ± 0.011	9.11% ± 3.10%	1.33 × 10 ¹⁴	6.30 × 10 ¹⁹
6 h	0.294 ± 0.041	0.078 ± 0.041	0.131 ± 0.004	25.57% ± 11.55%	1.55 × 10 ¹⁴	1.78 × 10 ²⁰
8 h	0.282 ± 0.036	0.131 ± 0.023	0.110 ± 0.014	46.39% ± 2.35%	1.48 × 10 ¹⁴	1.45 × 10 ²⁰
10 h	0.158 ± 0.046	0.100 ± 0.022	0.037 ± 0.004	64.31% ± 6.18%	8.29 × 10 ¹³	4.86 × 10 ¹⁹
12 h	0.097 ± 0.033	0.028 ± 0.011	0.056 ± 0.026	28.76% ± 2.20%	5.12 × 10 ¹³	5.69 × 10 ¹⁸
14 h	0.095 ± 0.026	0.025 ± 0.008	0.050 ± 0.009	25.85% ± 3.13%	5.00 × 10 ¹³	3.78 × 10 ¹⁸
18 h	0.070 ± 0.013	0.016 ± 0.007	0.043 ± 0.003	22.22% ± 6.46%	3.66 × 10 ¹³	3.39 × 10 ¹⁸
22 h	0.065 ± 0.015	0.014 ± 0.004	0.036 ± 0.001	23.36% ± 9.39%	3.43 × 10 ¹³	3.35 × 10 ¹⁸

^aFor each time point, MPI was extracted from 300 ml of cell-free supernatant or MVs collected from the same volume of culture supernatant. Experiments were repeated three times.

^bEquation: $\frac{\text{MPI amount in MVs (g)}}{\text{MPI amount in supernatant (g)}} \times 100$.

^cEquation: $\frac{\text{MPI amount (g/ml)} \times 6.02 \times 10^{23} \text{ (mol}^{-1}\text{)}}{1144.4 \text{ (g/mol)}}$.

^dEquation: $\frac{\text{MPI amount (g/ml)} \times 6.02 \times 10^{23} \text{ (mol}^{-1}\text{)} \times 10^{21}}{1144.4 \text{ (g/mol)} \times \frac{4}{3} \times \pi \times r \text{ (nm)}^3 \times \text{number of MVs (ml}^{-1}\text{)}}$.

and bacteria of the ΔS34-1 mutant lacked activity, as expected, the culture filtrate of the wild-type producer as well as wild-type bacteria produced considerable zones of lysis on the test plates (Figure 1b). Notably, when we applied pure MPI at the same concentration as determined to be present in the 4 × concentrated culture filtrate of the wild-type S34 producer (1.128 µg/ml; see Table 1), we could not detect any activity. (Note that activity of MPI in aqueous solution at low concentrations such as 0.5 µg/ml that we previously reported (Liu, Du et al., 2020) is only achieved when incubating with very low bacterial numbers.)

Then, we used 50-kDa cutoff filters to directly test whether MPI, which has a molecular weight of 1144.4 Da, is present in the S34-1 culture filtrate in monomeric or small oligomeric form as opposed to larger molecular weight forms. Of note, we verified that pure MPI completely passed through the 50-kDa filters that we used (Supplementary Figure S2). We monitored *S. aureus* growth in liquid culture after addition of the <50-kDa or >50-kDa fractions of *S. hominis* S34-1 or an equal volume of ΔS34-1 culture filtrate. Only the >50-kDa S34-1 culture filtrate fraction inhibited the growth of *S. aureus* (Figure 1c,d). These results show that MPI is not active or secreted in monomeric but in a larger molecular-weight form, which includes the possibility that it is associated with MVs.

3.2 | The MPI-producing organism secretes a considerable amount of MVs that persist during growth

To further investigate the possibility that MPI is associated with MVs, we first characterized MVs in the MPI-producing organism. To that end, we employed the “gold standard” method of MV purification that uses a final step of density-gradient ultracentrifugation after preparation of crude MVs using (i) harvesting of culture filtrate, (ii) 50-kDa cutoff membrane ultrafiltration, and (iii) an initial ultracentrifugation step (Dauros Singorenko et al., 2017). This we deemed crucial in our study as the end products obtained with many other, easier MV purification methods lacking density-gradient ultracentrifugation also contain other material, such as cellular debris or large protein aggregates, which may lead to a misinterpretation of MV association (Kulp & Kuehn, 2010). Furthermore, we increased the times of the ultracentrifugation and density gradient ultracentrifugation steps as compared to previous reports on MV isolation from staphylococci (Lee et al., 2009), from 3 to 8 h and 2 to 5 h, respectively, as we found that this led to considerably higher yield as determined by lipid content, protein content, and particle number (Supplementary Figure S3). Analysis by transmission electron microscopy (TEM) revealed the presence of distinct spherical structures with a bilayer membrane and electron-dense luminal contents characteristic for MVs (Figure 2a).

It has been reported that vesiculation and MV presence can be strongly influenced by growth phase (Klimentová & Stulík, 2015). In *S. aureus* for example, the staphylococcal species where MVs have previously been investigated, MVs are predominantly found during early growth and then rapidly disappear (Schlatterer et al., 2018; Wang et al., 2018). When we purified MVs from different time points during growth of *S. hominis* S34-1 and used protein content, lipid content, and particle abundance to estimate the MV amount, we consistently found a maximum of MV production between about 6 and 12 h of growth, which corresponds

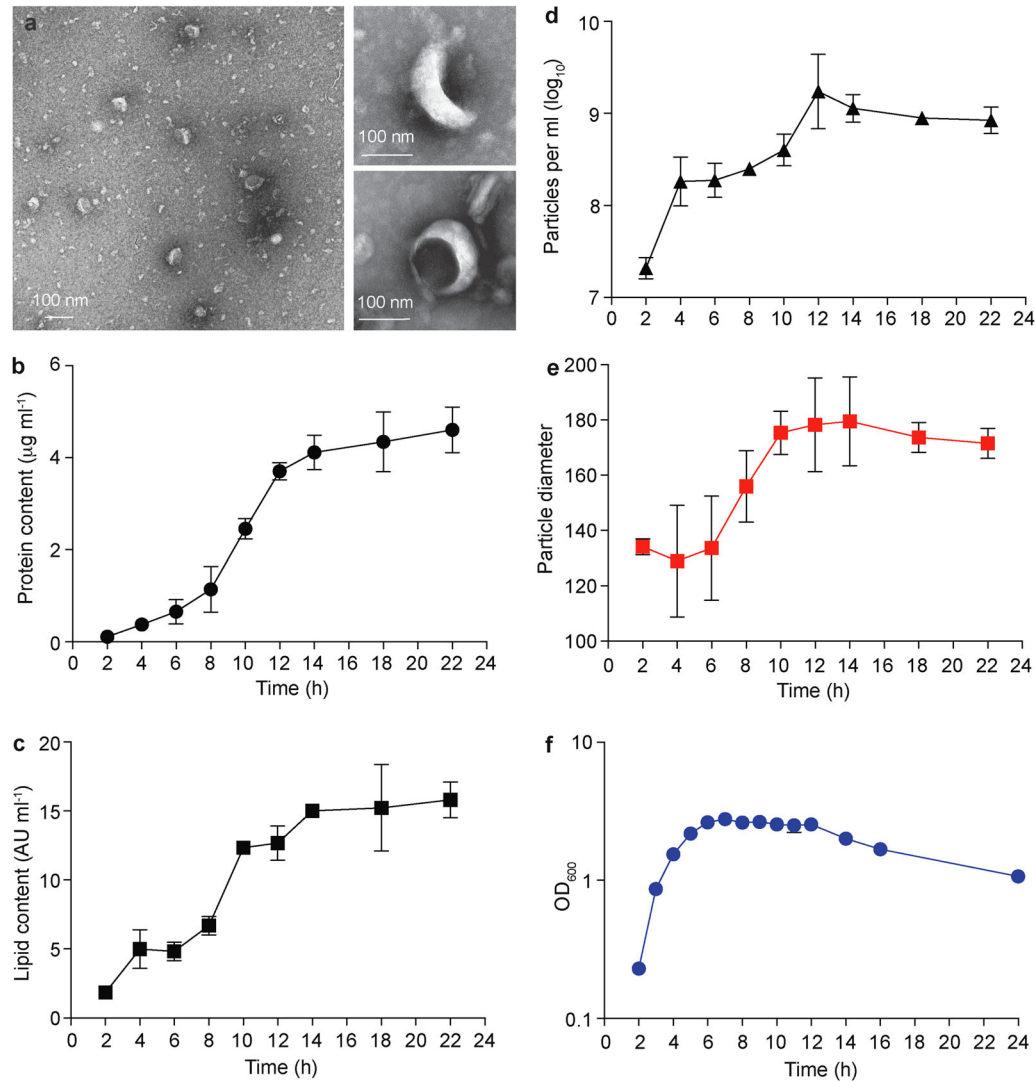


FIGURE 2 The MPI-producing organism secretes a considerable amount of MVs that persist during growth. (a) TEM of MVs prepared from *S. hominis* S34-1 culture filtrate. (b–e) Analysis of the indicated parameters in MVs prepared at each timepoint from 300 ml of *S. hominis* S34-1 culture filtrate. Data are presented per ml of initial culture volume. (f) Growth of the culture (OD_{600}). (b–e) $n = 3/\text{group}$. Error bars show the mean \pm SD

to the late phase of exponential and early phase of stationary growth. Furthermore, we found that the average diameter of MVs, which was similar to that generally reported in the literature for bacterial MVs (Brown et al., 2015), increased during the maximal production time between 6 and 12 h of growth and then remained constant (Figure 2b–f).

Our data show that MVs persisted until the end of the investigated time period (22 h). These findings reveal substantial production and long-term persistence of MVs in *S. hominis* S34-1, which is considerably different from what has been reported in *S. aureus* (Schlatteger et al., 2018; Wang et al., 2018) and in accordance with the idea of a particular function in that bacteriocin-producing strain.

3.3 | MPI is associated with MVs

To determine whether MPI is carried by MVs, we analyzed the fractions obtained by density-gradient ultracentrifugation for an association between MPI and MVs (Figure 3). The distribution of MVs as measured by particle number, lipid content, and protein content in the fractions aligned well with the inhibitory activity toward *S. aureus*. Specifically, fractions 1 and 2 had the highest particle number and lipid content and fraction 2 the highest protein content (Figure 3a–c). MVs were detected by TEM in fractions 1–3, with fraction 2 showing most MVs (Figure 3d), indicating that MVs were contained mostly in fraction 2. Fraction 2 also contained almost all MPI and inhibitory activity toward *S. aureus* (Figure 3e,f). In stark contrast, an equal amount of pure MPI applied to the same density-gradient ultracentrifugation procedure was found almost exclusively in fraction 10, at the

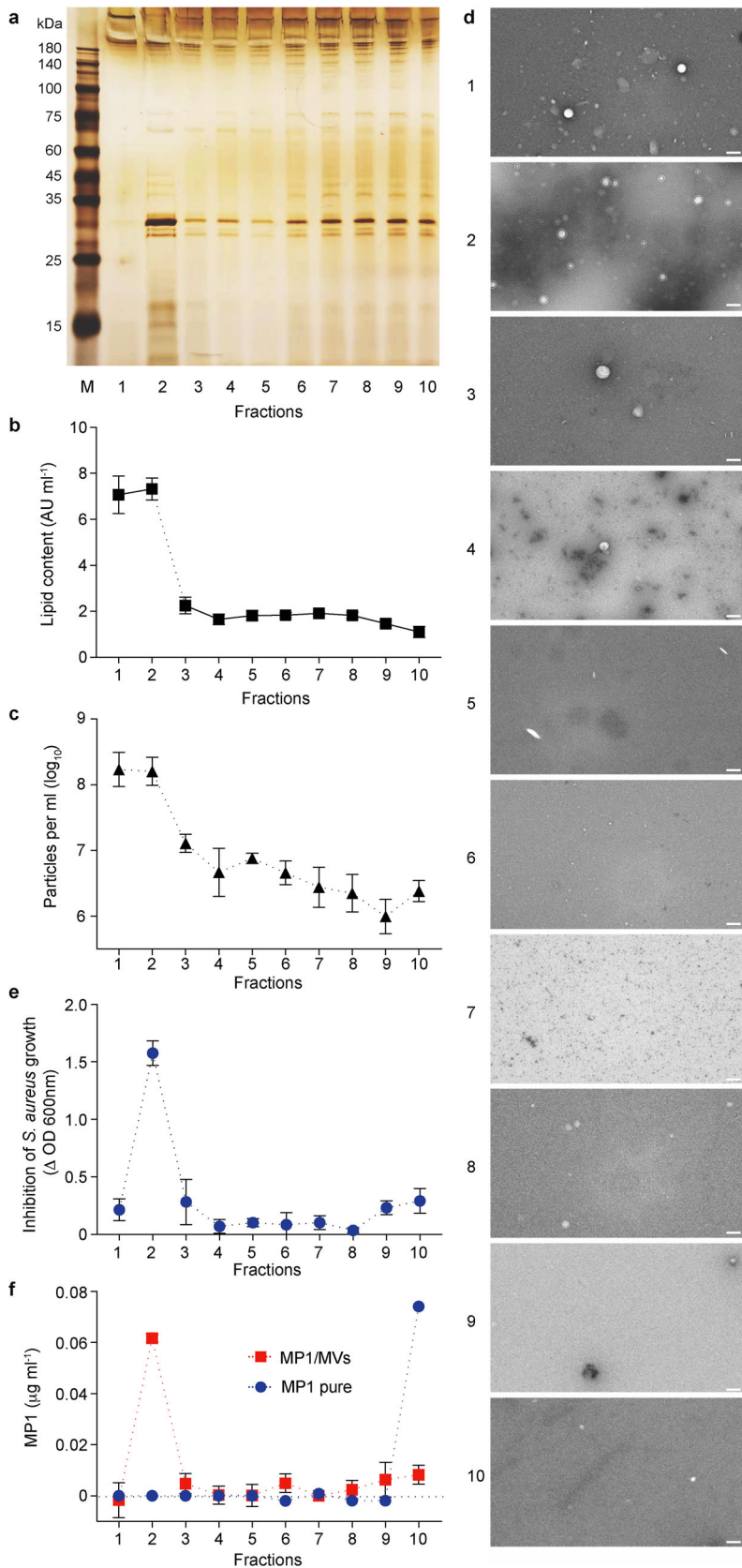


FIGURE 3 MPI is associated with the MV fraction in density gradient ultracentrifugation. Density gradient ultracentrifugation of crude MV preparations from *S. hominis* S34-1 culture filtrate was performed and fractions analyzed. (a) SDS-PAGE analysis of density gradient ultracentrifugation fractions. M, molecular weight marker. (b) Lipid content of fractions. $n = 3/\text{group}$. (c) Particle number in fractions. $n = 3/\text{group}$. (d) TEM pictures of fractions. Magnification is the same in all TEM pictures. Scale bar, 200 nm. (e) Inhibitory activity of fractions toward *S. aureus*, calculated by subtracting the corresponding OD₆₀₀ value of the S34-1 group from those of the ΔS34-1 group. $n = 3/\text{group}$. (f) MPI content per fraction. $n = 3/\text{group}$ (isolation from MVs). (b,c,f) Data are presented per ml of initial culture volume. Error bars show the mean \pm SD

very bottom of the ultracentrifugation tube, indicating aggregation to a high-density complex (Figure 3f). These results strongly indicate association of MP1 with MVs.

3.4 | MP1 becomes functional by MV association during growth

We then analyzed expression of the MP1 structural (*tcpE*) and selected biosynthesis genes (*tcpJ*, *tcpK*, *tcpL*) (Figure 4a) during growth, which showed a maximum of expression at ~4–6 h (Figure 4b), while MP1 protein concentration in the culture filtrate as measured by HPLC peaked slightly later, at 6–8 h (Figure 4c), in accordance with the gene expression timing. Later, overall MP1 amounts declined, probably due to proteolytic degradation by proteases, which are generally upregulated in staphylococci upon beginning of the late exponential growth phase (Le & Otto, 2015). The amount of MP1 that was associated with MVs peaked at 8 h, at which time it achieved ~46% of the total MP1 in the culture (Figure 4c, Table 1). Results from direct determination of soluble MP1 using 50-kDa cutoff filters were overall consistent with the data achieved for the MV-associated portion of MP1 in the culture filtrate (Table 1). The maximum percentage of MV-associated among total MP1 in the culture (~64%) was reached after 10 h of growth, after which it rapidly declined, likely due to cessation of MP1 gene expression and MV turnover, to remain at ~20–30% up to the last measured time point at 22 h (Figure 4c; Table 1).

Consistent with these data, several lines of evidence indicated high concentration of MP1 in MVs at 8 h of growth. First, the relative proportion of MP1 among all MV-associated proteins was maximal at 8 h (~12%) (Figure 4d). This measurement that was based on total protein assessment by a dye was also confirmed for the 8-h time point using HPLC, by comparing the MP1 peak area with the total area under curve, which also showed considerable MP1 relative amounts (210 nm absorption-based, 5.8%; 280 nm absorption-based, 4.8%), with somewhat lower values explainable by the fact that nonprotein components also absorb at those wavelengths (Figure 4e). Second, an estimation based on equal distribution of MP1 molecules and similar spherical sizes of MVs at the same cultivation time indicated remarkable concentration of MP1 in MVs, which exceeded that in the total culture filtrate at all time points by at least five orders of magnitude (Table 1). Of note, the degree of MV association of MP1 as determined by these methods is likely underestimated, because purification of MVs from culture filtrate does not have a 100% yield. The MP1-associated inhibitory activity (as measured by determination of the inhibitory activity of *S. hominis* S34-1 versus that of *S. hominis* ΔS34-1 toward cultures of *S. aureus*) was consistent in degree and kinetics in total culture filtrate, the >50 kDa-fraction of culture filtrate, and MVs, while the <50 kDa-fraction of culture filtrate lacked any such activity at any point during growth (Figure 4f). These data show that only the MV-associated form of MP1 in the culture has antimicrobial activity.

To assess the nature of MP1's association with MVs, we treated isolated MVs from the MP1-producing *S. hominis* S34-1 with proteinase K with or without previous treatment with beads to lyse the MVs (Supplementary Figure S4). Reduction of the total MP1 content by proteinase K without initial lysis would suggest that MP1 is only surface-attached on the MVs, while the need for initial lysis for MP1 to become vulnerable to proteinase K treatment would suggest that MP1 is embedded in the MVs. Treatment with proteinase K of lysed MVs led to a significant reduction of MP1, while only proteinase K or only bead-mediated lysis did not affect MP1 presence (Figure 5a). These results indicate that MP1 is an integral component of the MVs.

For MP1 to become embedded in MVs, two categorical possibilities exist: MP1 may be integrated in MVs before or during their synthesis and “budding” from the bacterial cell, or it may be secreted and then integrated into MVs. These two possibilities are difficult to address experimentally, due to our lack of knowledge about the exact mechanism of MV biosynthesis. While predicted dedicated export genes are not present in the MP1 biosynthesis locus of *S. hominis* S34-1, they are present in homologous gene clusters (Wieland Brown et al., 2009), suggesting that this family of bacteriocins is secreted generally by dedicated exporters. The genes responsible for MP1 export may be encoded elsewhere. The kinetics of MP1 association with MVs during growth that we detected, which show considerable amounts of non-MV associated MP1 in the first hours of growth and an increase of MV association from 2 to 10 h (Figure 4c; Table 1), suggest that MP1 becomes associated with MVs after being secreted independently, a scenario that appears possible given the hydrophobicity of MP1 and similar bacteriocins. To experimentally confirm that antimicrobially active, MV-embedded MP1 can be formed by association of external MP1 with MVs, we added MP1 to isolated, MP1-free MVs (obtained from *S. hominis* ΔS34-1). MVs were then isolated again and separated from soluble/external MP1, which showed presence of MP1 in the MVs as detected by their antimicrobial activity toward *S. aureus* (Figure 5b). We again used the proteinase K and bead lysis treatment to confirm that the externally added MP1 was integrated into rather than merely associated with MVs (Figure 5c). While association of MP1 with MVs before MV secretion from *S. hominis* producer cells cannot be excluded, together these data indicate that MVs are not essential for MP1 secretion and are in accordance with a model in which MP1 remains active after secretion by association with MVs. This is likely due to the membrane environment of MVs that allows higher concentrations of MP1 to remain soluble, while non-MV-associated MP1 forms inactive aggregates at concentrations exceeding the low solubility of MP1 (~1 μg/ml) in aqueous solutions (Chan & Burrows, 2021).

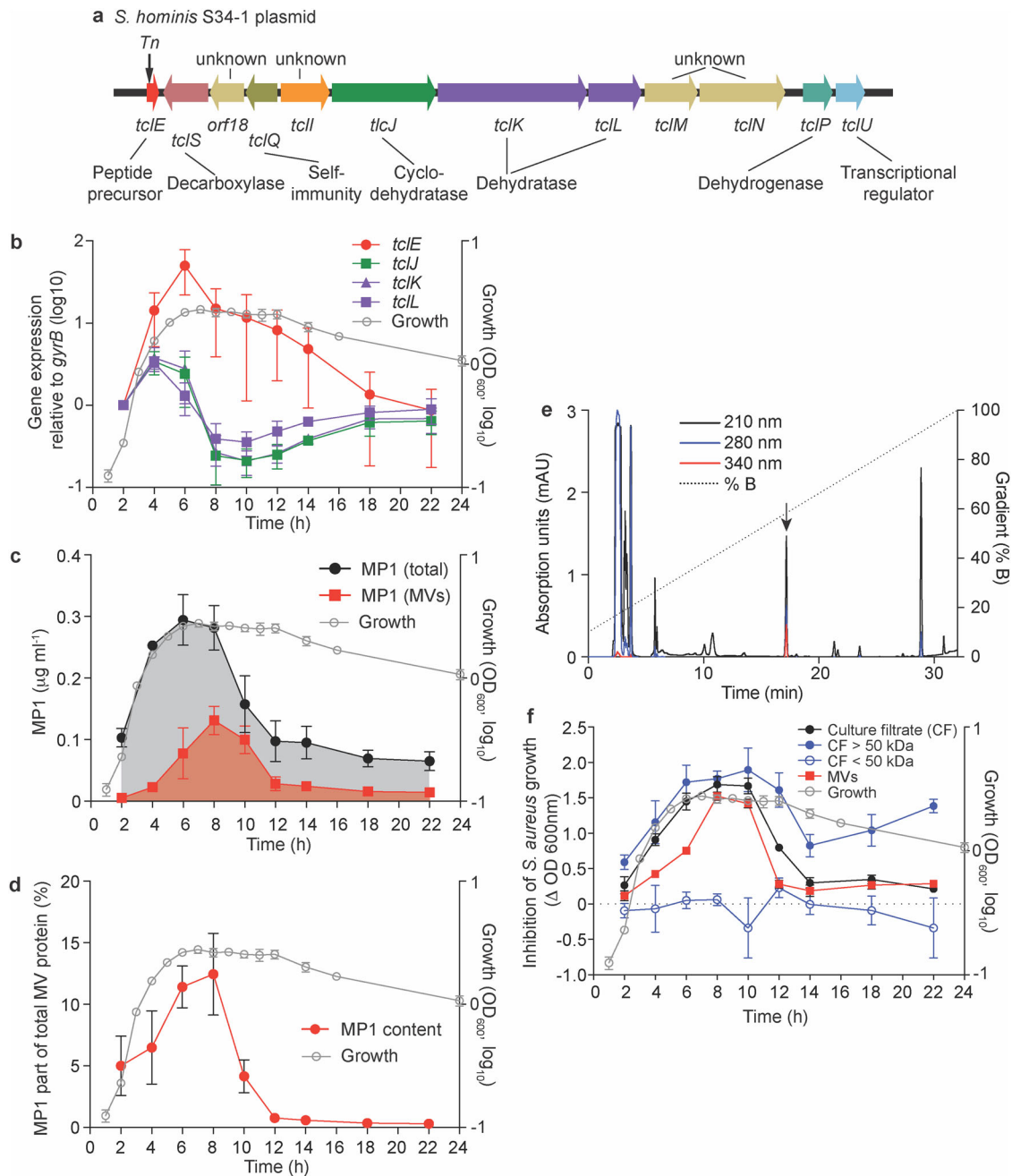


FIGURE 4 MPI becomes functional by MV association during growth. (a) The MPI biosynthetic locus in *S. hominis* S34-1. The structural gene is *tclE*. This gene carries a transposon insertion in strain Δ S34-1, abolishing production of MPI. Most genes in the locus perform enzymatic reactions involved in the post-translational modification of MPI. *tclQ* is involved in producer immunity. (b) Gene expression during growth as measured by qRT-PCR relative to the housekeeping gene *gyrB* of the MPI structural and selected biosynthetic genes. (c) MPI concentrations (determined by HPLC) in the culture filtrate (total) and the part associated with MVs during growth. Data are presented per millilitre of initial culture volume. (d) MPI portion of total protein contained in MVs during growth. (e) MPI content in MVs isolated after 8 h of growth by HPLC analysis. Shown are 210 and 280 nm wavelengths for estimation of total protein content (absorption of peptide backbone and aromatic amino acids, respectively) and 340 nm, where MPI has an absorption maximum. (f) Inhibitory activity toward *S. aureus* of total culture filtrate (supernatant of initial centrifugation step to remove cells), > and <50 kDa fractions of that supernatant as prepared by ultrafiltration with 50 kDa cutoff devices, and of MVs, during growth. (b–d,f) The corresponding growth curve (OD_{600}) is depicted with grey open circles and grey connecting lines and plotted on the right Y axis. $n = 3/\text{group}$. Error bars show the mean \pm SD

3.5 | MV-embedded MPI is delivered to the target cell via membrane fusion

It is not completely understood how bacterial MV components target other bacteria. OMVs from Gram-negative bacteria have been shown to fuse with eukaryotic cells (Bomberger et al., 2009; Kaparakis-Liaskos & Ferrero, 2015) and with OMVs of other Gram-negative bacteria (Kadurugamuwa & Beveridge, 1996). Gram-positive MVs are also known to associate with the surface

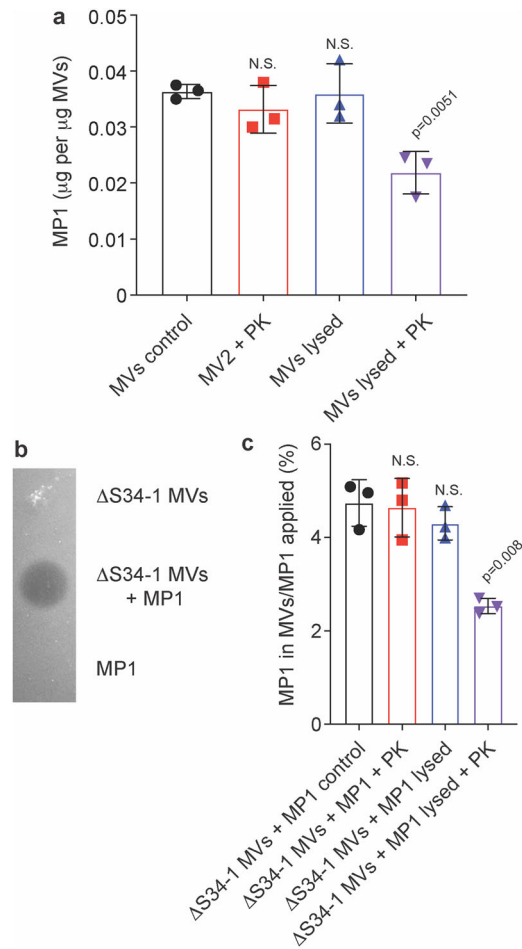


FIGURE 5 MPI is an internal component of MVs and may integrate into MVs from the external medium. (a) Effect of proteinase K (PK) with or without lysis by beads on MVs prepared from *S. hominis* S34-1. (See Supplementary Figure S4 for effects of bead treatment to lyse MVs.) The MPI content was determined after treatment by HPLC. (b) Antimicrobial activity toward *S. aureus* of original and MPI-exposed MVs of *S. hominis* ΔS34-1. (c) Proteinase K (PK) and bead lysis treatment of *S. hominis* ΔS34-1 MVs exposed to MPI (HPLC analysis). Data are expressed as percentage of total MPI applied, which was determined by HPLC of samples that were mixed with MVs but not separated by ultracentrifugation. (a, c) Statistical analysis is by 1-way ANOVAs and Dunnett's post-tests versus values obtained with the control. $n = 3/\text{group}$. Error bars show the mean \pm SD

of other bacteria (Kadurugamuwa & Beveridge, 1996), but whether this includes membrane fusion and how exactly components of MVs enter Gram positive bacterial target cells is not known.

Theoretically, MPI may enter the target cell after release from MVs in the vicinity of the target cell and diffusion through the membrane. Alternatively, the MPI-loaded MVs may fuse with the target cell membrane, which would ascertain delivery of the entire load and avoid solubility problems that would likely be encountered by external release. We therefore performed a series of experiments to investigate whether MPI-loaded MVs associate with, but also specifically whether they fuse with the target bacterial membrane. We included in these experiments, in addition to *S. aureus*, *Acinetobacter baumannii* as an exemplary Gram-negative bacterium as control.

We first examined whether MPI-loaded MVs deliver MPI to the target cell by assessing antimicrobial activity extracted from the target cells after association with MVs. Incubation of MVs from *S. hominis* S34-1, carrying MPI, resulted in MPI-mediated antimicrobial activity that could be extracted from *S. aureus*, indicating delivery of MPI via MVs to the *S. aureus* target cells (Figure 6a). In contrast, there was no antimicrobial activity in extracts from *A. baumannii* after association, indicating that MPI-loaded MVs cannot deliver MPI to that Gram-negative bacterium, most likely due to the presence of the outer membrane. This is noteworthy, as pure MPI also lacks activity toward Gram-negative bacteria, which is believed to be due to the inability of MPI to pass the outer membrane, except when specific receptors are present (Chan & Burrows, 2021).

To provide more direct evidence for an association of the MVs with the surface of *S. aureus*, we performed immuno-gold staining transmission electron microscopy (TEM) and fluorescence microscopy experiments. For TEM, MVs were first labeled with FITC and after incubation with cells, anti-FITC immuno-gold-labeled antibodies were used to visualize cell-associated MVs. *S. aureus*, but not *A. baumannii*, surfaces showed association with immuno-gold-labeled MVs (Figure 6b). For fluorescence

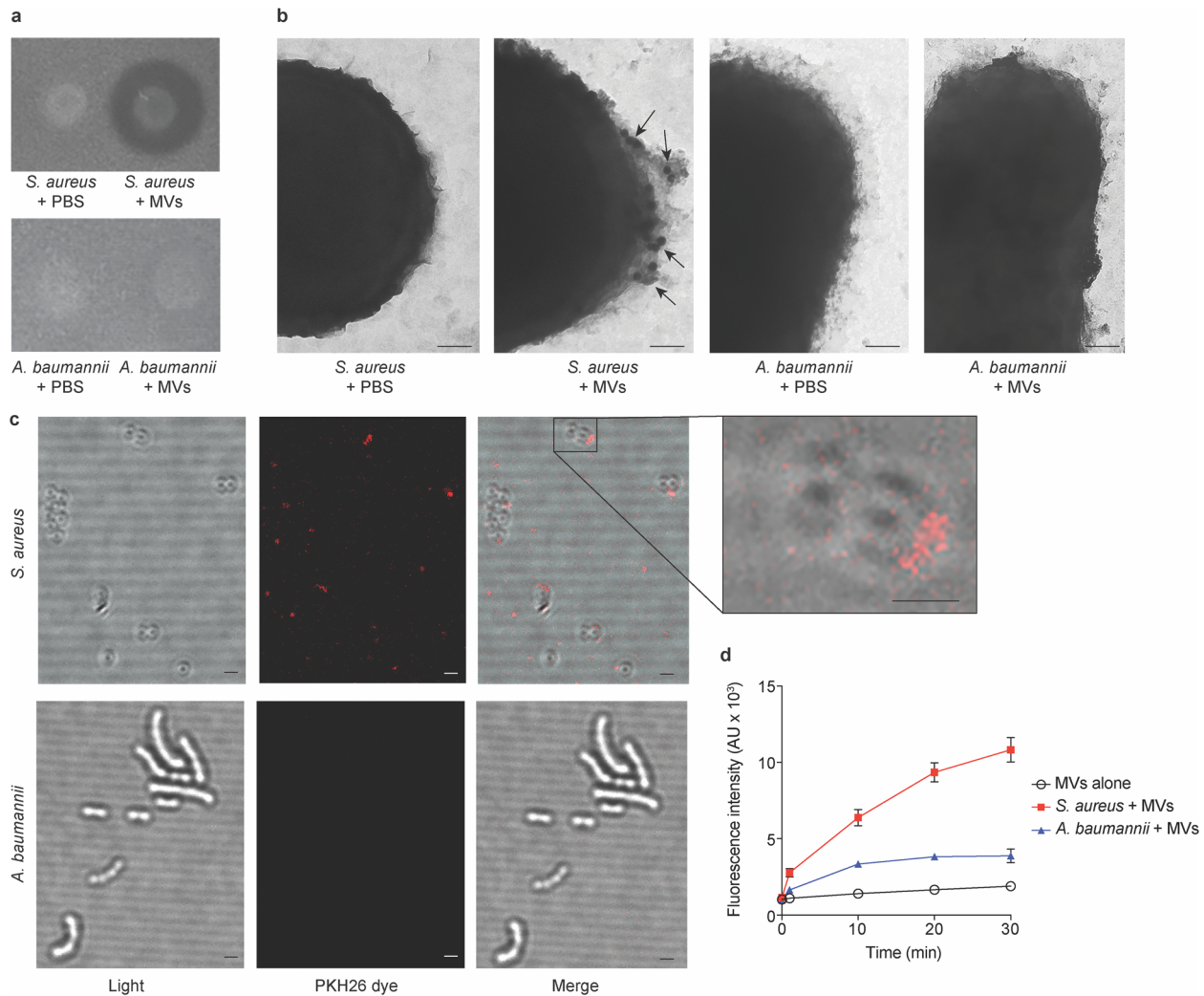
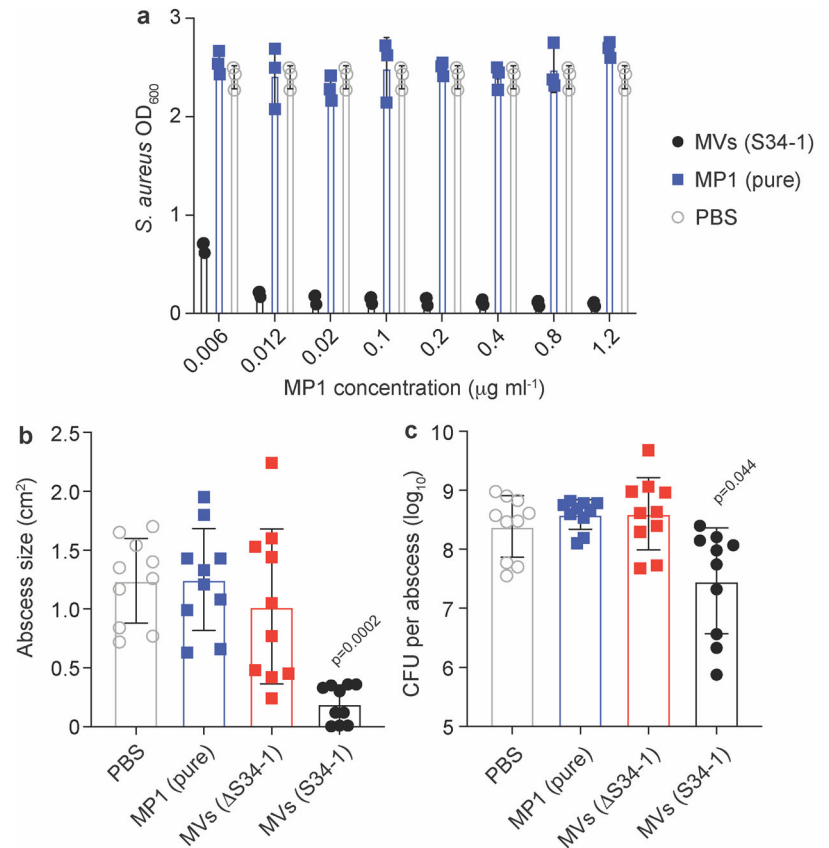


FIGURE 6 MVs associate with the surface and fuse with the cytoplasmic membrane of the target organism. (a) Delivery of MP-mediated antimicrobial activity by MVs to target bacteria. *S. hominis* S34-1 MVs were incubated with target bacteria (*S. aureus* or *A. baumannii*), cells were lysed, MP1 was extracted by ethyl acetate, and dried extracts redissolved in methanol were analyzed for antimicrobial activity on *S. aureus* test plates. (b) Analysis of surface association of immune-gold-labeled *S. hominis* S34-1 MVs with target bacteria. Scale bar, 100 nm. Arrows point to immune-gold-labeled particles. (c) Analysis of surface association by fluorescence microscopy. *S. hominis* S34-1 MVs were labeled with PKH26 dye and unbound dye was removed by ultracentrifugation (two times) and density-gradient ultracentrifugation. Labeled MVs were then incubated with target cells (37°C, 50 min), washed, and imaged using a confocal microscope. All scale bars, 1 μm. (d) Analysis of MV fusion with the target membrane. *S. hominis* S34-1 MVs were labeled with the self-quenching fluorescent dye R18 by incubation for 1 h, the dye was removed by ultracentrifugation and density-gradient ultracentrifugation, and the labeled MVs were incubated with target cells. $n = 3/\text{group}$. Error bars show the mean \pm SD

microscopy, MVs were labeled with PKH26, a highly fluorescent, lipophilic red dye that stains membranes by intercalation into the lipid bilayer. *S. aureus* cells were stained, suggesting association of MVs with cells, in contrast to *A. baumannii* (Figure 6c). High-resolution pictures indicated close association with the cell surface (Figure 6c). These results indicate that MVs closely associate with the surface of *S. aureus*.

While the TEM and fluorescence microscopy results indicated association of MVs with the surface of *S. aureus* cells, in similar fashion as shown before for the interaction of other MVs with bacterial targets (Tashiro et al., 2017), these experiments do not provide direct evidence for membrane fusion as opposed to mere association with the bacterial surface. Therefore, we used MVs labeled with octadecyl rhodamine B chloride (R18), a fluorescent dye that self-quenches when introduced into the lipid bilayer. An observed increase in fluorescence upon addition of MVs to *S. aureus* would indicate fusion with the cytoplasmic membrane due to the concomitant dilution effect and decrease of quenching. We observed a strong increase in fluorescence after addition of MVs to *S. aureus* in contrast to only a slight increase with *A. baumannii*, and no increase with a control, indicating that MVs from *S. hominis* S34-1 fuse with the cytoplasmic membrane of the sensitive *S. aureus* target bacteria (Figure 6d).

FIGURE 7 In-vitro and in-vivo activity of MP1 is strongly increased by MV association. (a) Direct comparison of corresponding concentrations of pure MP1 or MV-associated MP1 in assays measuring inhibition of *S. aureus* growth. Data are OD values obtained after 8 h of growth. See Supplementary Figure S5 for entire growth curves. $n = 3$ /group. (b) In-vivo mouse model of inhibition of *S. aureus* subcutaneous infection. Mice received equal amounts (600 ng) of pure or MV-associated MP1 from *S. hominis* S34-1 or Δ S34-1 as control 1 h after infection with 1×10^8 *S. aureus* CFU by injection into the infection site. Abscess sizes and CFU in the abscesses were determined 22 h afterward. $n = 10$ /group. Statistical analysis is by Kruskal-Wallis test with Dunn's multiple comparison test (b) and 1-way ANOVA with Dunnett's multiple comparison test (c) versus values obtained in the PBS control group. (b, c) Error bars show the mean \pm SD. See Supplementary Figure S6 for abscess pictures and measurement of inflammatory cytokines



3.6 | In-vitro and in-vivo activity of MP1 is strongly increased by MV association

Our results indicate that the antimicrobial efficacy of MP1 is dependent on MV association. To directly compare the degree by which MV association increases MP1 efficacy against *S. aureus* in vitro and in vivo, we first measured in-vitro activity of equal concentrations of MV-associated and pure MP1 against *S. aureus* growing in liquid culture up to the solubility of pure MP1 in aqueous solution ($\sim 1 \mu\text{g/ml}$). Pure MP1 was not active at any tested concentration, while considerable inhibition of the *S. aureus* target strain was already observed at a final concentration of $0.006 \mu\text{g/ml}$ of MV-associated MP1 (Figure 7a; Supplementary Figure S5). These results show that association of MP1 with MVs does not only overcome the low solubility of MP1, but increases antimicrobial efficacy compared to soluble MP1 by at least 2 logs.

Furthermore, we used a *S. aureus* subcutaneous infection model in which we injected pure MP1 or MV-associated MP1 at equal MP1 amounts (600 ng) 1 h after *S. aureus* injection. Injection of MV-associated MP1 but not pure MP1 resulted in significant reduction of CFU, abscess sizes, and inflammatory markers (Figure 7b; Supplementary Figure S6). These results indicate potency of MV-associated MP1, but not MP1 without MV association, in an in-vivo situation such as encountered during bacterial interaction.

4 | DISCUSSION

In nature, bacteria live in frequently competitive situations where they employ weapons of bacterial warfare to gain a survival benefit. Often, this is accomplished by the production of bacteriocins, which directly kill competitors (Riley & Wertz, 2002). Within the microbiome of the human skin and mucous epithelia, bacteriocins have been shown to be produced particularly by coagulase-negative staphylococci including *S. hominis*, to which they provide competitive advantages (Janek et al., 2016; Liu, Du et al., 2020; Nakatsuji et al., 2017; Zipperer et al., 2016). The mechanisms of action exerted by many bacteriocins require pronounced hydrophobicity, which poses a solubility problem as bacteriocins need to diffuse through an aqueous environment to reach the competing microorganisms. In the present study, we demonstrate how the producing bacteria manage to overcome this problem by incorporating a hydrophobic bacteriocin into MVs. Furthermore, we show that the bacteriocin is considerably concentrated in MVs and that MV association substantially increases antimicrobial activity beyond solely providing solubilization, which is likely due to optimized delivery in concentrated form to the target organism. Moreover, we provide evidence that MV

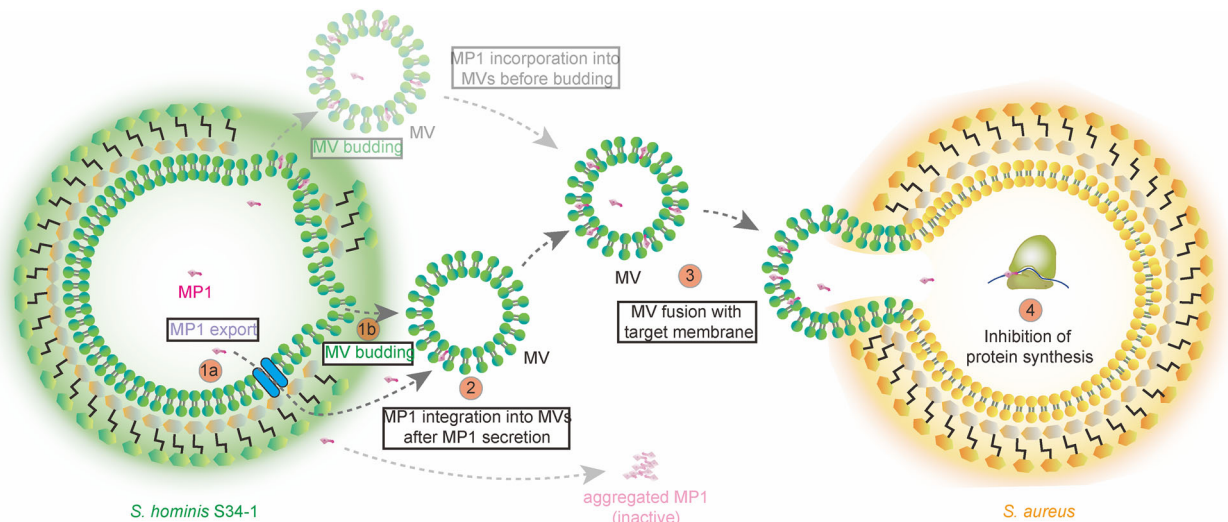


FIGURE 8 Model of essential role of MV association in bacteriocin-mediated bacterial competition. (a) The *S. hominis* S34-1 producer organism secretes the MPI bacteriocin and (b), produces MVs. 2, As results from this study suggest, MPI then becomes integrated in MVs. However, secretion of MVs with previously embedded MPI cannot be excluded as a possibility (depicted above). Non-MV-integrated MPI is inactive, likely forming precipitates due to low solubility. 3, MPI enters the target competing microorganism (*S. aureus* depicted as example) by fusion of the MVs with the competitor's membrane. 4, Inside the competitor, MPI exerts its known antimicrobial activity (by inhibition of association of the elongation factor G (EF-G) with the ribosome, inhibiting protein synthesis)

association also strongly increases activity in an animal model. Thus, our study shows that MV association renders an otherwise poorly active bacteriocin highly potent *in vitro* and *in vivo* (Figure 8).

The MV secretion process is not well understood and no dedicated and conserved MV production genes appear to exist (Brown et al., 2015; Kulp & Kuehn, 2010; Toyofuku et al., 2019). Likely, many factors participate in MV formation and they may also differ between bacterial strains. Furthermore, factors reportedly participating in MV biogenesis and secretion, such as autolysins in *B. subtilis* or the PSMs in *S. aureus*, have multiple additional roles in bacterial physiology (Abe et al., 2021; Cheung et al., 2014; Peschel & Otto, 2013; Schlatterer et al., 2018; Toyofuku et al., 2017; Vollmer et al., 2008; Wang et al., 2018). It is therefore not yet possible to use isogenic mutants to analyze the essentiality of MVs as for other bacterial factors. For that reason, we performed a thorough study of association between MVs and MPI activity. Multiple lines of evidence that we provide indicate the essentiality of MV incorporation for the activity of the studied bacteriocin MPI.

As for the putative mechanism of MPI secretion, our data suggest that MPI integrates into MVs after being exported by a yet unidentified exporter independently of MV formation. This notion is supported by the observed kinetics of MV-associated and MV-unassociated MPI concentration in the culture filtrate of the producer during growth, with high amounts of non-MV-associated MPI preceding presence of MV-associated MPI, and the fact that MPI homologues in other bacteria are known to be secreted by a dedicated exporter (Wieland Brown et al., 2009). In further support of this idea, we could demonstrate that non-MPI-containing MVs of *S. hominis* can be loaded with externally added MPI. However, secretion of MPI within budding MVs can certainly not be excluded as an additional mechanism contributing to MPI secretion.

It is poorly understood how bacteriocins or other MV-embedded molecules enter the target cell. This could be achieved by membrane fusion in a way similar to what has been described for the fusion of OMVs with eukaryotic host cells (Kaparakis-Liaskos & Ferrero, 2015) or, alternatively, by solubilization of MVs in close proximity to the target organisms' cell surface. Both mechanisms include challenges: membrane fusion requires passage of the MVs through the thick Gram-positive cell wall, which has often been described as a major mechanistic conundrum; however, the facts that MVs have been described recently in a number of Gram-positive bacteria (Cao & Lin, 2021) and that MVs penetrate the cell wall of the MPI-producing Gram-positive organism *S. hominis* suggest that this is possible. In further support of such a mechanism, recent structural studies have shown that staphylococcal cell walls contain channels that reach far through the cell wall (Pasquina-Lemonche et al., 2020). As for the alternative mechanism, release close to the cell surface, it has been shown that this happens in the case where cell-wall degrading enzymes associated with MVs have been attributed functions in bacterial competition (Kadurugamuwa & Beveridge, 1996). However, the target of those enzymes is in the extracellular space and for a substance such as MPI to reach its intracellular target, a dedicated importer or diffusion through the membrane would be needed. Our results demonstrate close association of MPI-loaded MVs with the target organism's surface and provide previously unavailable evidence for the fusion of MVs with the target cytoplasmic membrane. While we cannot exclude that some MPI molecules may diffuse through the target cytoplasmic membrane from the extracellular space, this is not likely to contribute significantly to the antibacterial activity of MPI, given its low solubility in aqueous solution. Notably, the fusion of MVs with the target cytoplasmic membrane that we demonstrate

here for MPI has not previously been demonstrated for Gram-positive bacterial targets and likely represents an efficient general mechanism to deliver MV-embedded molecules to such a target cell.

Our results not only give insight into how bacteria ensure activity of secreted hydrophobic bacteriocins, they also reveal that MVs can play essential rather than merely accessory roles in bacterial physiology. Most molecules found in MVs—such as toxins or enzymes—are soluble; and while MVs may increase the activity of those molecules due to concentrated delivery or fusion with the target cells, they are known to also be functional without MV association. Our study thus provides rarely obtained evidence for the notion that MVs in bacteria fulfil essential functions rather than representing, as previously suspected, an inconsequential by-product of bacterial growth and cell turnover without a dedicated role in bacterial physiology.

Our discovery raises interesting questions to be addressed in the future. For example, our results revealed that the MPI-producing organism, *S. hominis* S34-1, maintains MV production during growth for an extended time as compared to *S. aureus* strains in which growth-dependent MV production was previously assessed. *S. aureus* MVs can only be isolated from *S. aureus* at early growth stages, which has been explained by increased production during late exponential growth phase of the quorum sensing-controlled detergent-like PSM peptides believed to lyse MVs (Schlatterer et al., 2018). With different PSMs being produced by different staphylococcal species and strains (Cheung et al., 2014), this raises the question whether divergent growth phase-dependent MV presence in those bacteria is dependent on different PSM types or secretion characteristics. Furthermore, it is not yet clear how MPI is secreted. While our data are in support of a dedicated export system that remains to be identified and which exports MPI without MV association, clearly ruling out MV association for MPI export will only be possible once we are able to suppress MV formation by the deletion of specific MV biosynthesis-associated genes, if such genes exist.

In conclusion, our study shows how bacteria manage to keep a hydrophobic bacteriocin active during delivery through an aqueous environment to reach its target organism and how generally MV-embedded molecules can be delivered to the Gram-positive target cell by a membrane fusion mechanism. We believe that it is fair to assume based on the wide distribution of MVs that the activity of hydrophobic bacteriocins and possibly other hydrophobic substances is associated with MVs in similar form also in other bacteria. Furthermore, our findings provide rarely obtained evidence for the notion that MVs have essential functions in bacteria.

ACKNOWLEDGEMENTS

We thank the Central Lab of Ren Ji Hospital for their support in performing transmission electron microscopy and ultracentrifugation for this study. We also thank the Pharmaceutical Laboratory of Ren Ji Hospital for access to HPLC instruments. This work was supported by the innovative research team of high-level local universities in Shanghai, the National Natural Science Foundation of China (grant numbers 81873957, 82172325, to M.L.), the Shanghai Committee of Science and Technology, China (grant number 19JC1413005, to M.L.), and the Intramural Research Program of the National Institute of Allergy and Infectious Diseases (NIAID), U.S. National Institute of Health (NIH) (Project number ZIA AI000904, to M.O.).

CONFLICT OF INTEREST

The authors declare that they have no competing interests.

AUTHOR CONTRIBUTIONS

Conceptualization: M.O., M.L. Methodology: Y.L., M.L. Investigation: Y.L., Q.L., L.Z., H.W., R.X., T.C., Y.J., X.W., H.L. Visualization: Y.L., M.O. Funding acquisition: M.O., M.L. Supervision: M.L. Writing – original draft: M.L., M.O. Writing – review & editing: Y.L., S.W.D., M.O., M.L.

DATA AVAILABILITY STATEMENT

All data generated or analyzed during this study are included in this published article or in the supplementary information files.

ORCID

Michael Otto  <https://orcid.org/0000-0002-2222-4115>

REFERENCES

- Abe, K., Toyofuku, M., Nomura, N., & Obana, N. (2021). Autolysis-mediated membrane vesicle formation in *Bacillus subtilis*. *Environmental Microbiology*, 23, 2632–2647.
- Arthur, T. D., Cavera, V. L., & Chikindas, M. L. (2014). On bacteriocin delivery systems and potential applications. *Future Microbiology*, 9, 235–248.
- Bennallack, P. R., Burt, S. R., Heder, M. J., Robison, R. A., & Griffiths, J. S. (2014). Characterization of a novel plasmid-borne thiopeptide gene cluster in *Staphylococcus epidermidis* strain 115. *Journal of Bacteriology*, 196, 4344–4350.
- Bitto, N. J., Cheng, L., Johnston, E. L., Pathirana, R., Phan, T. K., Poon, I. K. H., O'Brien-Simpson, N. M., Hill, A. F., Stinear, T. P., & Kaparakis-Liaskos, M. (2021). *Staphylococcus aureus* membrane vesicles contain immunostimulatory DNA, RNA and peptidoglycan that activate innate immune receptors and induce autophagy. *Journal of Extracellular Vesicles*, 10, e12080.
- Bomberger, J. M., Maceachran, D. P., Coutermarsh, B. A., Ye, S., O'toole, G. A., & Stanton, B. A. (2009). Long-distance delivery of bacterial virulence factors by *Pseudomonas aeruginosa* outer membrane vesicles. *Plos Pathogens*, 5, e1000382.

- Brown, L., Wolf, J. M., Prados-Rosales, R., & Casadevall, A. (2015). Through the wall: Extracellular vesicles in Gram-positive bacteria, mycobacteria and fungi. *Nature Reviews Microbiology*, *13*, 620–630.
- Cao, Y., & Lin, H. (2021). Characterization and function of membrane vesicles in Gram-positive bacteria. *Applied Microbiology and Biotechnology*, *105*, 1795–1801.
- Caruana, J. C., & Walper, S. A. (2020). Bacterial membrane vesicles as mediators of microbe – microbe and microbe – host community interactions. *Frontiers in Microbiology*, *11*, 432.
- Chan, D. C. K., & Burrows, L. L. (2021). Thiocillin and micrococcin exploit the ferrioxamine receptor of *Pseudomonas aeruginosa* for uptake. *Journal of Antimicrobial Chemotherapy*, *76*, 2029–2039.
- Chan, D. C. K., & Burrows, L. L. (2021). Thiopeptides: Antibiotics with unique chemical structures and diverse biological activities. *The Journal of Antibiotics*, *74*, 161–175.
- Chatterjee, D., & Chaudhuri, K. (2011). Association of cholera toxin with *Vibrio cholerae* outer membrane vesicles which are internalized by human intestinal epithelial cells. *FEBS Letters*, *585*, 1357–1362.
- Cheung, G. Y. C., Joo, H. - S., Chatterjee, S. S., & Otto, M. (2014). Phenol-soluble modulins – Critical determinants of staphylococcal virulence. *FEMS Microbiology Review*, *38*, 698–719.
- Cho, I., & Blaser, M. J. (2012). The human microbiome: At the interface of health and disease. *Nature Reviews Genetics*, *13*, 260–270.
- Choi, S. Y., Lim, S., Cho, G., Kwon, J., Mun, W., Im, H., & Mitchell, R. J. (2020). *Chromobacterium violaceum* delivers violacein, a hydrophobic antibiotic, to other microbes in membrane vesicles. *Environmental Microbiology*, *22*, 705–713.
- Ciofu, O. (2000). Chromosomal beta-lactamase is packaged into membrane vesicles and secreted from *Pseudomonas aeruginosa*. *Journal of Antimicrobial Chemotherapy*, *4*, 9–13.
- Ciufolini, M. A., & Lefranc, D. (2010). Micrococcin PI: Structure, biology and synthesis. *Natural Product Reports*, *27*, 330–342.
- Dauros Singorenko, P., Chang, V., Whitcombe, A., Simonov, D., Hong, J., Phillips, A., Swift, S., & Blenkinsop, C. (2017). Isolation of membrane vesicles from prokaryotes: A technical and biological comparison reveals heterogeneity. *Journal of Extracellular Vesicles*, *6*, 1324731.
- Dean, S. N., Leary, D. H., Sullivan, C. J., Oh, E., & Walper, S. A. (2019). Isolation and characterization of *Lactobacillus*-derived membrane vesicles. *Science Reports*, *9*, 877.
- Ellis, T. N., & Kuehn, M. J. (2010). Virulence and immunomodulatory roles of bacterial outer membrane vesicles. *Microbiology and Molecular Biology Reviews*, *74*, 81–94.
- Faust, K., Sathirapongsasuti, J. F., Izard, J., Segata, N., Gevers, D., Raes, J., & Huttenhower, C. (2012). Microbial co-occurrence relationships in the human microbiome. *Plos Computational Biology*, *8*, e1002606.
- Fischetti, V. A. et al. (2019). *Gram-positive pathogens*. American Society for Microbiology.
- Grein, F., Schneider, T., & Sahl, H. -G. (2019). Docking on lipid II-A widespread mechanism for potent bactericidal activities of antibiotic peptides. *Journal of Molecular Biology*, *431*, 3520–3530.
- Héchar, Y., & Sahl, H. -G. (2002). Mode of action of modified and unmodified bacteriocins from Gram-positive bacteria. *Biochimie*, *84*, 545–557.
- Human Microbiome Project, C. (2012). Structure, function and diversity of the healthy human microbiome. *Nature*, *486*, 207–214.
- Janeč, D., Zipperer, A., Kulik, A., Krismer, B., & Peschel, A. (2016). High frequency and diversity of antimicrobial activities produced by nasal *Staphylococcus* strains against bacterial competitors. *Plos Pathogens*, *12*, e1005812.
- Kadurugamuwa, J. L., & Beveridge, T. J. (1996). Bacteriolytic effect of membrane vesicles from *Pseudomonas aeruginosa* on other bacteria including pathogens: Conceptually new antibiotics. *Journal of Bacteriology*, *178*, 2767–2774.
- Kaparakis-Liaskos, M., & Ferrero, R. L. (2015). Immune modulation by bacterial outer membrane vesicles. *Nature Reviews Immunology*, *15*, 375–387.
- Klimentová, J., & Stulík, J. (2015). Methods of isolation and purification of outer membrane vesicles from gram-negative bacteria. *Microbiological Research*, *170*, 1–9.
- Koepfen, K., Hampton, T. H., Jarek, M., Scharfe, M., Gerber, S. A., Mielcarz, D. W., Demers, E. G., Dolben, E. L., Hammond, J. H., Hogan, D. A., & Stanton, B. A. (2016). A novel mechanism of host-pathogen interaction through sRNA in bacterial outer membrane vesicles. *Plos Pathogens*, *12*, e1005672–e1005672.
- Kulp, A., & Kuehn, M. J. (2010). Biological functions and biogenesis of secreted bacterial outer membrane vesicles. *Annual Review of Microbiology*, *64*, 163–184.
- Le, K. Y., & Otto, M. (2015). Quorum-sensing regulation in staphylococci—an overview. *Frontiers in Microbiology*, *6*, 1174.
- Lee, E. - Y., Choi, D.-Y., Kim, D. - K., Kim, J. - W., Park, J. O., Kim, S., Kim, S. - H., Desiderio, D. M., Kim, Y. - K., Kim, K. - P., & Gho, Y. S. (2009). Gram-positive bacteria produce membrane vesicles: Proteomics-based characterization of *Staphylococcus aureus*-derived membrane vesicles. *Proteomics*, *9*, 5425–5436.
- Lekmetchai, S., Su, Y.-C., Brant, M., Alvarado-Kristensson, M., Vallström, A., Obi, I., Arnqvist, A., & Riesbeck, K. (2018). *Helicobacter pylori* outer membrane vesicles protect the pathogen from reactive oxygen species of the respiratory burst. *Frontiers in Microbiology*, *9*, 1837.
- Li, M., Dai, Y., Zhu, Y., Fu, C. - L., Tan, V. Y., Wang, Y., Wang, X., Hong, X., Liu, Q., Li, T., Qin, J., Ma, X., Fang, J., & Otto, M. (2016). Virulence determinants associated with the Asian community-associated methicillin-resistant *Staphylococcus aureus* lineage ST59. *Science Reports*, *6*, 27899.
- Liu, Q., Meng, H., Lv, H., Liu, Y., Liu, J., Wang, H., He, L., Qin, J., Wang, Y., Dai, Y., Otto, M., & Li, M. (2020). *Staphylococcus epidermidis* contributes to healthy maturation of the nasal microbiome by stimulating antimicrobial peptide production. *Cell Host Microbe*, *27*, 68–78.e5 e65.
- Liu, Y., Du, Z., Zhang, L., Chen, J., Shen, Z., Liu, Q., Qin, J., Lv, H., Wang, H., He, L., Liu, J., Huang, Q., Sun, Y., Otto, M., & Li, M. (2020). Skin microbiota analysis-inspired development of novel anti-infectives. *Microbiome*, *8*, 85.
- Mashburn, L. M., & Whiteley, M. (2005). Membrane vesicles traffic signals and facilitate group activities in a prokaryote. *Nature*, *437*, 422–425.
- Moll, G. N., Konings, W. N., & Driessen, A. J. M. (1999). Bacteriocins: Mechanism of membrane insertion and pore formation. *Antonie Van Leeuwenhoek*, *76*, 185–198.
- Nakatsuji, T., Chen, T. H., Narala, S., Chun, K. A., Two, A. M., Yun, T., Shafiq, F., Kotol, P. F., Bouslimani, A., Melnik, A. V., Latif, H., Kim, J.-N., Lockhart, A., Artis, K., David, G., Taylor, P., Streib, J., Dorrestein, P. C., Grier, A., ... Gallo, R. L. (2017). Antimicrobials from human skin commensal bacteria protect against *Staphylococcus aureus* and are deficient in atopic dermatitis. *Science Translational Medicine*, *9*, eaah4680.
- Niaz, T., Shabbir, S., Noor, T., & Imran, M. (2019). Antimicrobial and antibiofilm potential of bacteriocin loaded nano-vesicles functionalized with rhamnolipids against foodborne pathogens. *LWT - Food Science and Technology*, *116*, 108583.
- Paharik, A. E., Parlet, C. P., Chung, N., Todd, D. A., Rodriguez, E. I., Van Dyke, M. J., Cech, N. B., & Horswill, A. R. (2017). Coagulase-negative *Staphylococcus* strain prevents *Staphylococcus aureus* colonization and skin infection by blocking quorum sensing. *Cell Host Microbe*, *22*, 746–756.e5 e745.
- Pasquina-Lemonche, L., Burns, J., Turner, R. D., Kumar, S., Tank, R., Mullin, N., Wilson, J. S., Chakrabarti, B., Bullough, P. A., Foster, S. J., & Hobbs, J. K. (2020). The architecture of the Gram-positive bacterial cell wall. *Nature*, *582*, 294–297.
- Peschel, A., & Otto, M. (2013). Phenol-soluble modulins and staphylococcal infection. *Nature Reviews Microbiology*, *11*, 667–673.
- Riley, M. A., & Wertz, J. E. (2002). Bacteriocins: Evolution, ecology, and application. *Annual Review of Microbiology*, *56*, 117–137.

- Schlatterer, K., Beck, C., Hanzelmann, D., Lebtig, M., Fehrenbacher, B., Schaller, M., Ebner, P., Nega, M., Otto, M., Kretschmer, D., & Peschel, A. (2018). The mechanism behind bacterial lipoprotein release: Phenol-soluble modulins mediate toll-like receptor 2 activation via extracellular vesicle release from *Staphylococcus aureus*. *mBio*, 9, e01851-18.
- Schwechheimer, C., & Kuehn, M. J. (2015). Outer-membrane vesicles from Gram-negative bacteria: Biogenesis and functions. *Nature Reviews Microbiology*, 13, 605–619.
- Tashiro, Y., Hasegawa, Y., Shintani, M., Takaki, K., Ohkuma, M., Kimbara, K., & Futamata, H. (2017). Interaction of bacterial membrane vesicles with specific species and their potential for delivery to target cells. *Frontiers in Microbiology*, 8, 571.
- Towle, K. M., & Vederas, J. C. (2017). Structural features of many circular and leaderless bacteriocins are similar to those in saposins and saposin-like peptides. *Medchemcomm*, 8, 276–285.
- Toyofuku, M., Cárcamo-Oyarce, G., Yamamoto, T., Eisenstein, F., Hsiao, C. - C., Kurosawa, M., Gademann, K., Pilhofer, M., Nomura, N., & Eberl, L. (2017). Prophage-triggered membrane vesicle formation through peptidoglycan damage in *Bacillus subtilis*. *Nature Communication*, 8, 481.
- Toyofuku, M., Morinaga, K., Hashimoto, Y., Uhl, J., Shimamura, H., Inaba, H., Schmitt-Kopplin, P., Eberl, L., & Nomura, N. (2017). Membrane vesicle-mediated bacterial communication. *The ISME Journal*, 11, 1504–1509.
- Toyofuku, M., Nomura, N., & Eberl, L. (2019). Types and origins of bacterial membrane vesicles. *Nature Reviews Microbiology*, 17, 13–24.
- Vollmer, W., Joris, B., Charlier, P., & Foster, S. (2008). Bacterial peptidoglycan (murein) hydrolases. *Fems Microbiology Review*, 32, 259–286.
- Wang, S., Gao, J., & Wang, Z. (2019). Outer membrane vesicles for vaccination and targeted drug delivery. *Wiley Interdisciplinary Reviews: Nanomedicine and Nanobiotechnology*, 11, e1523–e1523.
- Wang, X., Thompson, C. D., Weidenmaier, C., & Lee, J. C. (2018). Release of *Staphylococcus aureus* extracellular vesicles and their application as a vaccine platform. *Nature Communication*, 9, 1379.
- Wieland Brown, L. C., Acker, M. G., Clardy, J., Walsh, C. T., & Fischbach, M. A. (2009). Thirteen posttranslational modifications convert a 14-residue peptide into the antibiotic thiocillin. *Proceedings of the National Academy of Sciences of the United States of America*, 106, 2549–2553.
- Woyke, T., Teeling, H., Ivanova, N. N., Huntemann, M., Richter, M., Gloeckner, F. O., Boffelli, D., Anderson, I. J., Barry, K. W., Shapiro, H. J., Szeto, E., Kyrpides, N. C., Musmann, M., Amann, R., Bergin, C., Ruehland, C., Rubin, E. M., & Dubilier, N. (2006). Symbiosis insights through metagenomic analysis of a microbial consortium. *Nature*, 443, 950–955.
- Zipperer, A., Konnerth, M. C., Laux, C., Berscheid, A., Janek, D., Weidenmaier, C., Burian, M., Schilling, N. A., Slavetinsky, C., Marschal, M., Willmann, M., Kalbacher, H., Schitteck, B., Brötz-Oesterhelt, H., Grond, S., Peschel, A., & Krismer, B. (2016). Human commensals producing a novel antibiotic impair pathogen colonization. *Nature*, 535, 511–516.

SUPPORTING INFORMATION

Additional supporting information may be found in the online version of the article at the publisher's website.

How to cite this article: Liu, Y., Liu, Q., Zhao, L., Dickey, S. W., Wang, H., Xu, R., Chen, T., Jian, Y., Wang, X., Lv, H., Otto, M., & Li, M. (2022). Essential role of membrane vesicles for biological activity of the bacteriocin micrococcin P1. *Journal of Extracellular Vesicles*, 11, e12212. <https://doi.org/10.1002/jev2.12212>